Heterogenized molecular (pre)catalysts for water oxidation and oxygen reduction

Ham, C.J.M. van der

1 | Introduction

"Advice is a dangerous gift, even from the wise to the wise, and all courses may run ill."

J.R.R. Tolkien in *The Fellowship of the Ring*

1.1 Renewable energy and its storage

1.1.1 The energy problem and catalysis

Between 400,000 B.C. and 1950, the global carbon dioxide concentration in the atmosphere has been fluctuating.[1] The highest value for the estimated CO_2 concentration in that period is approximately 300 ppm.[1] As a consequence of the use of fossil fuel the carbon dioxide concentration in the atmosphere has increased far beyond the natural fluctuations observed before 1950. Currently the CO_2 concentration is somewhat above 400 ppm while the emission of CO_2 is still increasing annually.[2, 3] The increase in global CO_2 concentration is the major cause of global climate change.[4]

In order to limit the global temperature increase, more renewable energy sources need to be employed. Solar energy and wind energy are promising alternatives for the traditional fossil fuels.[5, 6] One of the big challenges of renewable energy that needs to be faced before implementation is the large-scale storage of this renewable energy. Batteries are good energy carriers for low energy applications. However, the transportation of energy stored in batteries for large scale applications is cumbersome. Moreover batteries in general are not very environmentally friendly due to the presence of heavy metals such as lead. Storage of energy in a chemical fuel *e.g.* has the advantage of forming a full cycle in which no waste products are formed. The storage of energy as a chemical fuel therefore is an interesting alternative to the use of batteries in for example the automotive industry.

The reduction of protons and CO_2 to chemical fuels such as hydrogen and hydrocarbons has received a lot of attention lately.[7–12] The proton reduction reaction (PRR) to produce hydrogen and the hydrogen oxidation reaction (HOR) to consume hydrogen are shown in Equation 1.1.[7–11]

$$2\,H^+ + 2\,e^- \underset{\text{HOR}}{\overset{\text{PRR}}{\rightleftharpoons}} H_2 \tag{1.1}$$

A generalized reaction scheme for the reduction of CO_2 is displayed in Equation 1.2

$$CO_2 + n\,H^+ + n\,e^- + 2\,e^- \rightleftharpoons CO + \text{hydrocarbons} + \text{alcohols} + m\,H_2O \tag{1.2}$$

An electrochemical cell consists of two halfreactions, thus a second halfreaction is needed

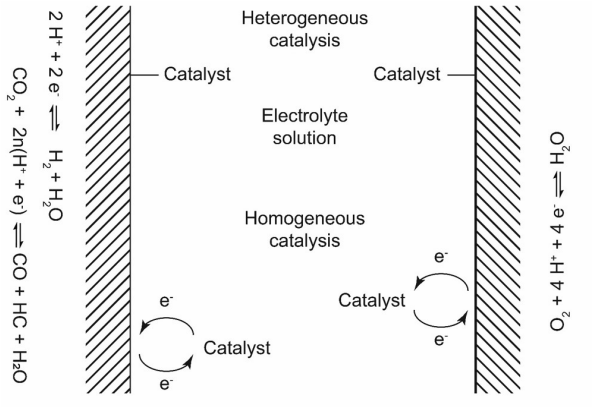

Figure 1.1: Schematic representation of heterogeneous (top part) and homogeneous (bottom part) catalysts as used in an electrochemical cell, HC = hydrocarbons.

to complement the PRR/HOR halfreaction. The water oxidation reaction (WOR) and oxygen reduction reaction (ORR) are good reactions to complement the PRR/HOR (see Equation 1.3), thus forming a closed cycle of two half reactions. The high redox potential (1.23 V *versus* RHE) and the non-toxicity of water and oxygen formed makes this redox reaction very suitable to in combination with the PRR and HOR redox reaction. The oxygen can be released into the atmosphere during fuel production. The waste products of the consumption of the renewable fuels produced 1.1 and 1.2 are water (in Equation 1.1 and 1.2) and CO_2 (in Equation 1.2 only). Both water and CO_2 are non-toxic products. Water is harmless for the environment whereas the CO_2 produced upon the oxidation of alcohols and hydrocarbons is captured from the atmosphere when these fuels are produced, so net no CO_2 is produced. In order to increase the rate and efficiency of the redox reactions, efficient catalysts are needed.

$$O_2 + 4\,H^+ + 4\,e^- \underset{\text{WOR}}{\overset{\text{ORR}}{\rightleftharpoons}} 2H_2O \tag{1.3}$$

In 1901, Ostwald discerned four different types of catalysis. In a 1902 publication in Nature, he stated: "*Catalytic action may be divided in four classes:-(1) Release in supersaturated systems. (2) Catalysis in homogeneous mixtures. (3) Heterogeneous catalysis. (4) Enzyme reactions.*".[13] The first process later became known as crystallization and is thus a physical phenomenon and not

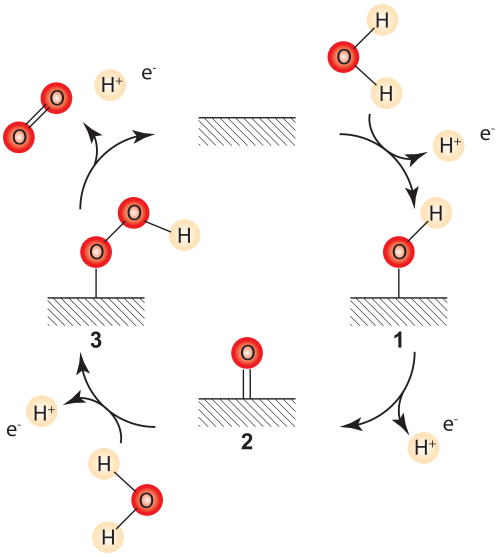

Figure 1.2: The most common mechanism for the electrochemical oxidation of water on heterogeneous surfaces.[15]

chemical nor catalytic.[14] In water oxidation and oxygen reduction catalysis, the focus is mostly on heterogeneous and homogeneous catalysis. Both have different traits and thus different advantages and disadvantages. In heterogeneous catalysis, the catalyst is in a different phase as the reactants. In electrocatalysis this means that the heterogeneous catalyst is the electrode itself or at least attached to the electrode surface (top part of Figure 1.1). Heterogeneous catalysts can be quite stable but are limited in opportunities for design. In homogeneous catalysis the catalyst and the reactant are in the same solution phase (bottom part of Figure 1.1). This means that in homogeneous electrocatalysis the electrode is only transferring electrons to or from the catalyst which is dissolved in the (aqueous) electrolyte and situated in very close proximity to the electrode. Homogeneous catalysts are generally more easy to tune than heterogeneous catalysts, but in general lack in stability.

1.1.2 Heterogeneous catalysts for the electrochemical oxidation of water

Heterogeneous electrocatalysis for the water oxidation and oxygen reduction reactions is a much more explored field compared to homogeneous electrocatalysis.[16–19] In the most common model, the first step in the heterogeneous water oxidation mechanism is the binding of the water molecule to a vacant site on the metal-oxide surface where it is oxidized and deprotonated, forming a metal hydroxide (Figure 1.2, **1**). This hydroxide is further oxidized and deprotonated forming a oxo-species (**2**). The oxo-species undergoes an attack by water and deprotonation and oxidation of the water molecule forming a superoxo-species (**3**). The superoxo-species is deprotonated and oxidized and dioxygen is liberated from the electrode surface (**4**).

The equilibrium potential for the water oxidation reaction ($E^0_{O_2/H_2O}$) is 1.23 V *versus* RHE.[20] From this equilibrium potential the free energy of a dioxygen molecule can be calculated when the free energy of water is defined as zero (Equations 1.4 and 1.5).[20]

$$e_0 E^0_{O_2/H_2O} = C_0 = [\Delta G(O_2) - \Delta G(H_2O)]/4 = 1.23\ \text{eV} \tag{1.4}$$

$$\Delta G(O_2) = 4 \times C_0 = 4.92\ \text{eV} \tag{1.5}$$

The optimal water oxidation catalyst for the heterogeneous oxidation of water should fulfill the condition wherein the intermediates **1**, **2** and **3** have an increased metal binding energy of 1.23 eV per reaction step (Equations 1.6-1.8).[20]

$$\Delta G(OH_{Ads}) = C_0 = 1.23\ \text{eV} \tag{1.6}$$

$$\Delta G(O_{Ads}) = 2 \times C_0 = 2.46\ \text{eV} \tag{1.7}$$

$$\Delta G(OOH_{Ads}) = 3 \times C_0 = 3.69\ \text{eV} \tag{1.8}$$

The scaling relations describe that the binding energy of all intermediates are connected, due to the similarity in the manner in which the intermediates are bound to the catalyst, as was first described in the group of Nørskov.[21] This means that it is not possible to optimize the binding energy of the intermediates to the electrode surface individually. The difference in binding energy of the OH_{Ads} and OOH_{Ads} species is 3.2 ± 0.2 eV on flat (111) surfaces, which is higher than the optimal 2.46 eV (Figure 1.3).[22] This non-optimal difference in binding energy between the

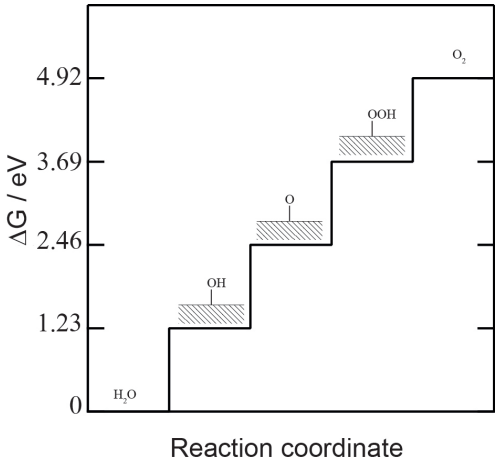

Figure 1.3: Intermediates in heterogeneous water oxidation reaction with their optimal binding energy. The arrow indicates the minimum binding energy difference for OH_{Ads} and OOH_{Ads}, which is 3.2 eV instead of the thermodynamic 2.46 eV due to scaling relations.

OH_{Ads} and OOH_{Ads} species leads to an additional potential that needs to be applied above the equilibrium potential of 1.23 V *versus* RHE for the water oxidation reaction. The extra potential that needs to be applied above the equilibrium potential to start catalysis is called the overpotential. In Figure 1.3 the energy levels of the intermediates are displayed *versus* the reaction coordinate under ideal circumstances. The steps which form the bottleneck of 3.2 eV *versus* the ideal 2.46 eV are indicated by the arrow.

The group of Jaramillo reported a benchmarking study for the water oxidation reaction wherein different surface metal oxide deposits on glassy carbon electrodes were investigated in alkaline media.[19] The potential was measured while water oxidation was performed chronoamperometrically at 10 mA cm^{-2} based on the geometric surface area. The metal oxide surfaces under consideration consisted of (alloys of) Co, La, Fe, Ir, Ni and Ce. IrO_2 was the best performing electrocatalyst with a potential of 1.55 V *versus* RHE at 10 mA cm^{-2}. The best performing non-noble metal catalyst was shown to be $NiFeO_x$ with a reported potential of 1.58 V *versus* RHE at 10 mA cm^{-2}. The potential for all non-noble metal catalyst are similar at 10 mA cm^{-2} between 1.58

and 1.66 V *versus* RHE. The IrO_2 catalyst has a lower potential at 10 mA cm^{-2}, but is unstable during long term electrolysis. However, in acidic electrolyte, the potential and thus the activity of IrO_2 was stable over 2 hours at 1.6 V *versus* RHE, whereas the non-noble metal based catalysts lost their activity.

1.1.3 Homogeneous catalysts for the (electro)chemical oxidation of water

For the homogeneous oxidation of water two different mechanisms are predominantly described in literature.[23] The first mechanism is similar to the mechanism for heterogeneous catalysts for water oxidation (Figure 1.2). In homogeneous context this mechanism is called the water nucleophilic attack (WNA) mechanism. The only difference between the heterogeneous and homogeneous mechanisms is that the electrode surface, depicted by the hatched rectangle in Figure 1.2, is replaced with the metal center of the molecular catalyst (M). Homogeneous catalytic systems following the WNA mechanism suffer from the same scaling relations and intrinsic overpotential as their heterogeneous counterparts. The difference in binding energy between each intermediate to the metal center needs to be equal to 1.23 eV (Equations 1.6-1.8). However the energy difference between the M-OH and M-OOH intermediates will be around 3.2 eV instead of the ideal 2.46 eV, leading to an intrinsic overpotential before water oxidation catalysis starts.

The other mechanism predominantly reported in literature starts with two metal binding sites which bind water and go through two deprotonation and oxidation steps, forming two metal-oxo species (Figure 1.4).[15] These two metal-oxo species couple via a radical reaction, dioxygen is released and the free binding sites on the two metal centers are available for a new catalytic cycle. This mechanism is called the radical oxo coupling (ROC) mechanism. In the ROC mechanism the optimal catalyst is found when $\Delta G_{M\text{-}OH}$ = 1.23 eV and $\Delta G_{M\text{-}O\bullet}$ = 2.46 eV, similarly to the WNA mechanism.[15] The potential limiting factor in catalysts displaying the WNA mechanism is the non-optimal $\Delta G_{M\text{-}OH} - \Delta G_{M\text{-}OOH}$ energy difference of at least 3.2 eV. Since there is no M-OOH intermediate in the ROC catalytic cycle, this bottleneck does not exist in the ROC mechanism, which might lead to catalysts with a lower overpotential.

The first report of a molecular water oxidation catalyst was by Meyer *et al* in 1982 (Figure 1.5, top left).[24] They reported a ruthenium-based $[(bpy)_2(H_2O)RuO\text{-}Ru(H_2O)(bpy)_2](ClO_4)_4$ complex (bpy = 2,2'-bipyridine) which evolves oxygen both electrochemically in acidic electrolyte

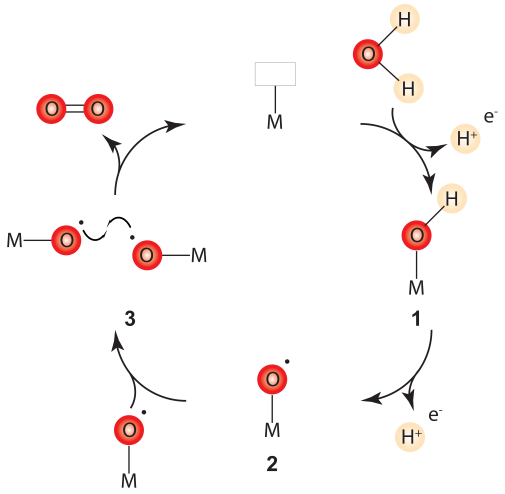

Figure 1.4: Radical oxo coupling (ROC) mechanism for certain homogeneous water oxidation catalysts.

and by chemical oxidation using cerium(IV) as chemical oxidant. A multitude of molecular complexes as catalysts for the water oxidation reaction has been reported since then. In the group of Sun, severak Ru-based molecular complexes have been developed as catalysts for both chemical and photochemical water oxidation (Figure 1.5, top right).[25] The complex [Ru(bda)(isoq)$_2$] (H_2bda = 2,2'-bipyridine-6,6'-dicarboxylic acid; isoq = isoquinoline) was used as catalyst to oxidize water using cerium(IV) or $[Ru(bpy)_3]^{2+}$ and light. A ROC mechanism was proposed wherein a ruthenium(IV) peroxo-dimer is formed.[26] Liberation of oxygen is the rate-limiting step under stoichiometric amounts of cerium(IV). Under excess of cerium(IV), oxygen liberation happens after the peroxo-dimer is further oxidized to form a superoxo-dimer and the rate determining step changes to the formation of the peroxo-dimer.

The first iridium-based molecular catalyst for the water oxidation reaction was reported by the group of Bernhard (Figure 1.5, bottom left).[27] A series of different cyclometallated iridium complexes was studied under chemical oxidation conditions and shown to perform water oxidation, forming dioxygen as the product. Since then different iridium-based catalysts for the water oxidation reaction have been reported.[28–30] Under electrocatalytic conditions some of

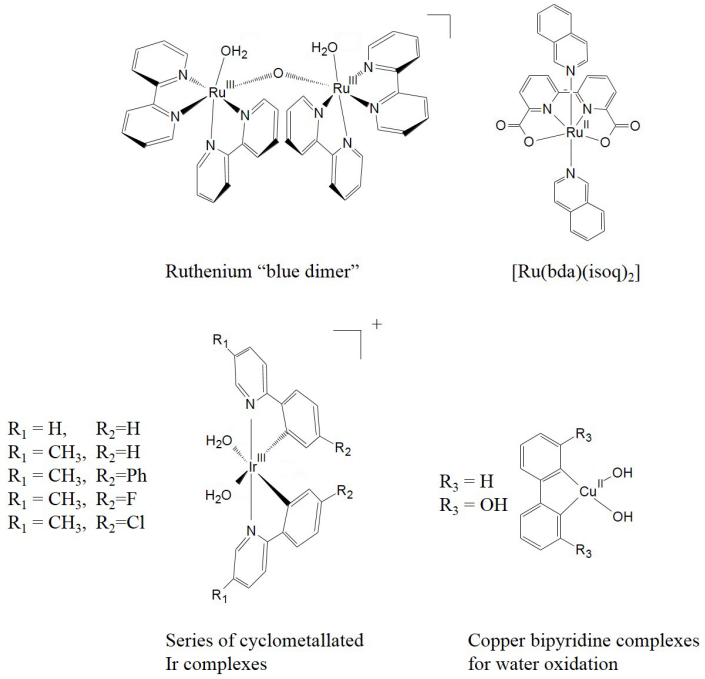

Figure 1.5: Examples of molecular complexes used in (electro)chemical water oxidation and oxygen reduction studies.

those complexes form a IrO_2 deposit on the electrode surface.[31–33] In electrocatalytic studies of molecular iridium complexes it is therefore a challenge to prevent the formation of iridium oxide layers on the electrode surface.

1.1.4 Copper complexes for the electrochemical water oxidation and oxygen reduction reaction.

Molecular copper electrocatalysts have been reported both for the water oxidation reaction and oxygen reduction reaction.[34–40] The first reported copper-based water oxidation catalyst is a copper bipyridine system which forms a mononuclear bishydroxy complex at high pH (Figure 1.5, bottom right).[39] Water oxidation catalysis was observed in a pH range of 11.6 to 13.3. A turnover frequency of 100 s^{-1} is reported at glassy carbon electrodes. Quickly after, a sec-

ond report on homogeneous water oxidation from the group of Lin appeared, wherein a 6,6'-dihydroxy-2,2'-bipyridine ligand was used. It has a lower overpotential and higher activity than the 2,2'-bipyridine complex, which is attributed to the proton shuttling effect of the hydroxy groups present on the bipyridine ligand. A number of copper based complexes have been reported for the oxygen reduction reaction with phenanthroline derivative ligands and its derivatives,[41–43] and pyridylalkylamine ligands.[44, 45] In homogeneous copper catalysis the challenge lies in finding catalysts that do not form heterogeneous copper (oxide) layers instantaneously on the electrode surface. This is due to the fast ligand exchange kinetics of copper, which may lead to the formation of free copper ions in the electrolyte solution.[46] Nevertheless, in literature the formation of heterogeneous metal (oxide) catalysts under reaction conditions is rarely discussed.

1.2 The thin line between homogeneous and heterogeneous catalysis

1.2.1 Degradation of homogeneous catalysts

Pinpointing the active species can be a challenge in homogeneous catalysis, as often only the resting states of the catalytic species are detectable, whereas the true active species are only present in undetecteable concentrations.[14] Since molecular catalyst have a lower stability than heterogeneous catalysts, catalyst degradation can be a major problem. In a 2011 review, Crabtree gave an overview of how homogeneous species may degrade during a catalytic reaction and how one may recognize the formation of nanoparticles.[14] The most important indications of the formation of heterogeneous catalysts from homogeneous species are summarized in Table 1.1.[14] One should always keep in mind the possibility of forming a heterogeneous catalyst from a homogeneous complex.

1.2.2 The difficulty in determining the active species in electrochemical homogeneous catalysis

The thin line between homogeneous and heterogeneous catalysis as discussed in the previous section also holds for electrochemical studies. Under oxidative conditions the formation of metal

Table 1.1: *Suspicious circumstances suggesting a need for further study of an operationally homogeneous metal catalyst system, adapted from Crabtree.[14]*

Events	**Comment**
Unexplained lag time before onset of catalysis	Conversion of molecular precursor to an active catalyst, possibly nanoparticulate
Catalyst properties, such as selectivity, closely resemble the properties of the appropriate analogous conventional heterogeneous catalyst	Nanoparticle (NP) catalysis possible
Ligand (L) effects are minimal; all active catalysts have similar rates and properties	All catalysts may convert to NPs having similar catalytic properties whatever the nature of L, but ligands can modify NP synthesis and so ligand-dependent activity cannot eliminate the possibility that NPs are the active species
Catalytic activity is halted by a selective poison for the heterogeneous catalyst	Hg(0) is most common but precautions are needed
Kinetic irreproducibility	Nanoparticle synthesis can be very dependent on conditions
Reaction mixture turns dark in color	Possible indication of NPs
Metal-containing deposit or mirror formed	Possible indication of intermediacy of NPs, and the deposit itself may be catalytically active
Harsh conditions	Ligands may degrade and release metal

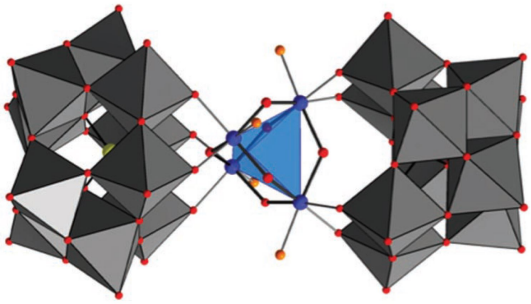

Figure 1.6: Structure of the ruthenium based POM **1** as reported simultaneously in the groups of Hill ([49]) and Bonchio ([50]). Depicted is the central $Ru_4(\mu\text{-}O)_4(\mu\text{-}OH)_2(H_2O)_4{}^{6+}$ core (ball-and-stick representation, Ru blue, μ-O red- O(H_2) orange; hydrogen atoms omitted for clarity) and the slightly distorted Ru_4 tetrahedron (transparent blue). The polytungstate fragments are shown as gray octahedra, and Si as yellow spheres. The figure was reprinted from [49].

oxides from coordination compounds has been observed, whereas under reductive conditions the formation of a metallic layer is a possibility. The difficulty of interpretation of the data and the care with which the experimental conditions should be chosen is greatly displayed in the study of Co-based polyoxometallates (POMs) as water oxidation catalysts described by the groups of Hill [47] and Finke.[48] Both argued on the specification of the active species of these POM systems. Since these systems have been discussed in so many details, and since the same problems are likely to arise for other systems, it is presented here as a case study.

Polyoxometallate compounds are carbon-free ligands that can bind to metal ions, for example ruthenium. The ruthenium-based POM $Rb_8K_2[Ru_4O_4(OH)_2(H_2O)_4(\gamma{-}SiW_{10}\text{-}O_{36})_2]\cdot 25H_2O$ (**1**) was developed simultaneously in the groups of Bonchio[50] and Hill[49]. In the group of Hill, it was shown to oxidize water using both $[Ru(bpy)_3]^{3+}$[49, 51] and $(NH_4)_2[Ce(NO_3)_6]$ (CAN)[51] as chemical oxidant. Experiments using isotopically labelled water showed the formation of dioxygen from water and not from oxygen present in **1**.[49] Control experiments were performed with $[RuCl_3]$, which forms RuO_2 under catalytic conditions. The $RuCl_3$ catalyst showed an activity two orders of magnitude lower than that of **1**, indicating the complex does not degrade into RuO_2 during catalysis. The rate limiting step for water oxidation was determined to be the first oxidation

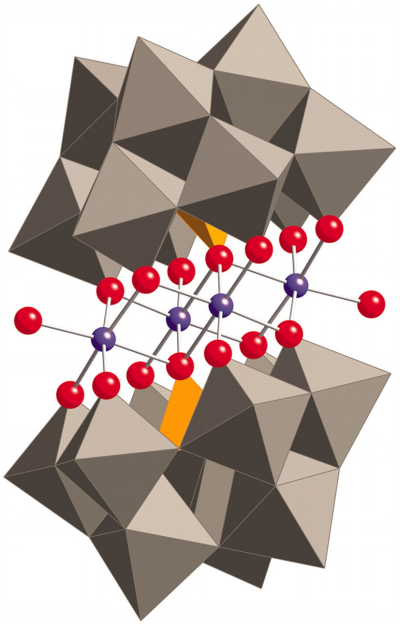

Figure 1.7: X-ray structure of Na_{10}**2** in combined polyhedral ($[PW_9O_{34}]$ ligands) and ball-and-stick (Co_4O_{16} core) notation. Co atoms are purple; O/OH_2(terminal) are red; PO_4 is displayed as orange tetrahedrals; and WO_6 as gray octahedra. Hydroge natoms, water molecules, and sodium cations are omitted for clarity. Figure reprinted from [47].

of water from the four times oxidized complex.[51] The complex is stable in water from neutral to slightly acidic pH, but will decompose below a pH of 1.5.[49]

Simultaneously in the group of Bonchio, the same polyoxometallate was developed and investigated using CAN.[50] Oxygen evolution was confirmed using gas chromatography and maximum turn over frequencies of 450 h^{-1} were observed. The catalyst was precipitated from the aqueous solution after water oxidation by addition of CsCl. Infrared and Raman spectroscopy of the precipitated complex confirmed the stability of the catalyst.

After this ruthenium-based POM compound, Hill reported the first Co_4-POM as active water oxidation catalyst.[47] The POM compound $[Co_4(H_2O)_2(PW_9O_{34})_2]^{10-}$ (**2**, Figure 1.7) was claimed to be an active water oxidation catalyst using both chemical and electrochemical oxidation. It was the only cobalt-based POM in a series to exhibit water oxidation using $[Ru(bpy)_3]^{3+}$.

A total turn over number (TON) of 75 was observed with a yield of 64%, based on the amount of $[Ru(bpy)_3]^{3+}$ added to the reaction solution. It was stated the catalyst could be kept in solution for 72 hours prior to catalysis without a significant change in TON and yield. At pH 8 a solution containing 5 μM **2** could be kept in water for over a month without changes in the ^{31}P NMR and the UV-Vis spectra. Nevertheless there is a concern that small amounts of Co^{2+} are responsible for the catalytic activity. By addition of bpy to to the solution, any free Co^{2+} in solution could be scavenged to form an inactive complex.[47] Some decrease in water oxidation activity is observed, which is attributed to loss of Co^{II} from the POM by competitive coordination of bpy and the oxidation of bpy. After the chemical oxidation by $[Ru(bpy)_3]^{3+}$ was completed, more $[Ru(bpy)_3]^{3+}$ was added to the catalyst solution. The same initial activity was observed in the second addition of $[Ru(bpy)_3]^{3+}$ as in the first addition, indicating no catalyst degradation took place during the first catalytic run.

By replacing the $[Ru(bpy)_3]^{3+}$ with the reduced form $[Ru(bpy)_3]^{2+}$ and with the addition $Na_2S_2O_8$ as sacrificial reductant, light-activated water oxidation was performed with **2** as catalyst.[52] An increase in both catalytic as well as initial quantum yield was observed with increasing catalyst concentration at pH 8. The highest TON of 224 was observed at 5 μM, the highest concentration used in this report.

Stracke and Finke continued the investigation of **2** electrochemically.[48] By performing a long-term cyclic voltammetry experiment with 500 μM solutions of **2** at pH 8 between 1.47 and 1.87 V *versus* RHE, the behavior of the catalyst over time was investigated at a 0.071 cm^2 glassy carbon (GC) electrode. The onset for water oxidation is observed around 1.65 V *versus* RHE. At the beginning of the experiment, the current reaches a maximum of 11 μA at the vertex potential of 1.86 V. Over time the maximum current increases to 140 μA after 3 hours of cycling. Such an activation process indicates a transformation of the molecular species and possibly deposition of material on the electrode surface. Scanning electron microscopy (SEM) in combination with energy dispersive X-ray spectroscopy (EDX) confirmed the presence of a cobalt layer on the surface of the GC electrode. The layer contained Co, O, P, and Na, with a Co:P:Na ratio of approximately 4:1:1, as determined by EDX. No tungsten from the PW_9O_{34} moiety was observed in the deposit. The CoO_x layer could also be formed by applying an oxidizing potential of 1.76 V *versus* RHE for 30 minutes. By transferring the electrode with deposit to an electrolyte solution in the absence of

2, the catalytic activity was retained. This suggests that the catalytic activity should be attributed to the surface adsorbed CoO_x.

The formation of the CoO_x layer under electrochemical conditions led to a further investigation of the catalytically active catalytic species under photochemical circumstances by Sartorel, Scandola and co-workers.[53] Using nanosecond flash photolysis, a 50 μM solution of $[Ru(bpy)_3]^{2+}$ was transformed (partly) into $[Ru(bpy)_3]^{3+}$. Depletion of the $[Ru(bpy)_3]^{3+}$ by reduction by a 5 μM solution of **2** was measured in the μs timescale using UV-Vis. As the catalyst was aged for longer times before photolysis, depletion of $[Ru(bpy)_3]^{3+}$ was faster, indicating that a decomposition product formed *in situ* is responsible for the depletion of $[Ru(bpy)_3]^{3+}$. As the oxidation of pristine **2** in cyclic voltammetry is higher than the oxidation potential of $[Ru(bpy)_3]^{3+}$, (photo)chemical water oxidation of **2** should not be possible with $[Ru(bpy)_3]^{2+}$ as oxidatant. The timescales wherein the $[Ru(bpy)_3]^{3+}$ is depleted does point to a molecular species, as the timescales are similar to stable Ru-POMs and is about 3 orders of magnitude higher than *e.g.* colloidal IrO_2 particles.[53, 54]

The concentration of **2** used in the electrochemical investigation by Stracke and Finke[48] is two orders of magnitude higher (0.5 mM) than the reports from Hill *et al* (<5 μM).[47, 52] An investigation of the maximum absorption of the 580 nm peak in UV-Vis spectroscopy of a 0.5 mM solution of **2** in 0.1 M phosphate buffer at pH 8 shows a decrease of 4.6 $\pm$ 0.6% over 3 hours.[48] This indicates that **2** degrades over time at high concentration. This was further confirmed with linear-sweep voltammetry based on the anodic peak at 1.77 V *versus* RHE at pH 8, which is associated with the presence of free Co^{II} in solution. The total amount of free Co^{II} leached was established electrochemically to be 58 μM after 3 hours, which corresponds to 2.9% of the total amount of cobalt added to the solution.

A further chemical and photochemical investigation of low concentration (<5 μM) of **2** in borate buffer at pH 8, once again showed the active catalyst is the completely intact Co_4-POM, with little to no activity from solvated Co^{II}.[55] Using UV-Vis spectroscopy, it was established that **2** is unstable in phosphate buffer, the buffer used in all reports described above, but is much more stable in borate buffer. Using ICP-MS and cathodic adsorptive stripping voltammetry (CAdSV) experiments a sixfold higher concentration of dissolved cobalt in phosphate buffers over borate buffers was observed. Photochemical water oxidation in the presence of **2** reached a turn over

number of 302 at pH 8, which is much higher than the TON reported for **2** in phosphate buffer. A chemical dioxygen yield of 24.2% was observed in borate buffer at pH 8.

The debate about the homogeneity or heterogeneity of the POM **2** is reviewed in the 2013 *JACS* paper of Geletii, Hill and co-workers concluding: "catalytic studies of molecular species, especially POM WOCs (water oxidation catalysts), under one set of experimental conditions should be compared only with extreme caution, if at all, to those under other conditions."[55]

After the initial 2010 Science paper from the group of Hill,[47] another Co-POM catalyst was reported with $Na_{10}[Co_4(H_2O)_2(VW_9O_{34})_2]\cdot 35H_2O$ (Na_{10}**3**$\cdot 35H_2O$) from the same group in 2014.[56] An exceptionally high TOF of $> 1 \times 10^3$ was observed under chemical oxidation conditions, based on the consumption of $[Ru(bpy)_3]^{3+}$. The catalyst is also active towards light driven water oxidation with $[Ru(bpy)_3]^{2+}$ and $Na_2S_2O_8$ as sacrificial reductant. Multiple spectroscopic techniques were used to establish the stability of the complex in solution and under catalytic conditions. In the ^{51}V NMR spectrum a peak was observed at -506.8 ppm, which does not change over the course of a month.

The stability and structure of the Na_{10}**3**$\cdot 35H_2O$ was questioned in the group of Finke.[57] The synthesis of Na_{10}**3**$\cdot 35H_2O$ yielded a brown powder, of which the elemental analysis was too high in tungsten by 1.56 %.[56, 57] In the synthesis of Na_{10}**3**$\cdot 35H_2O$ by Finke *et al* NaOAc impurities were found which were identified using infrared spectroscopy.[57] The infrared spectra reported by the group of Hill were cut off at 1200 cm^{-1}, well below the peak associated with NaOAc which is observed at 1600 cm^{-1} A critical note was also set at the ^{51}V NMR shift of -508.6 ppm with regard to the nature of that peak. Due to **3** being quadrupolar in vanadium, one would expect this peak to be broad. In **3**, a sharp peak with $\delta\nu_{1/2}$ = 28 Hz is observed at -508.6 ppm[56] or -510 ppm.[57] This is narrower than for any tetrahedral vanadium complex reported to date. Previously $V_4O_{12}{}^{4-}$ was reported to have the narrowest peak with $\delta\nu_{1/2}$ = 60 Hz.[57] If the procedure for synthesis of **3** is followed, but without the addition of the Co^{II} salt the -510 ppm is retained in the ^{51}V NMR spectrum. This indicates the -510 or -508.6 ppm peak is not associated with the complexated form of **3** claimed by Hill and coworkers,[56] but rather with the *cis*-$V_2W_4O_{19}{}^{4-}$ ligands which are dissociated from the cobalt center.[57] Purification of Na_{10}**3**$\cdot 35H_2O$ by recrystallization yielded a green solid which was determined to be mostly *cis*-$V_2W_4O_{19}{}^{4-}$

Electrochemical water oxidation using the Na_{10}**3**$\cdot 35H_2O$ catalyst was performed by Folkman and Finke both in phosphate and in borate buffer.[58] In the first hour of catalysis the oxidation current increases for both phosphate and borate buffers present in the electrolyte solution. The formation of a CoO_x layer is observed on the electrode surface as was confirmed with SEM/EDX. The ease of formation of CoO_x is attributed to free Co^{II}_{aq} dissolved in the electrolyte solution from the decomposition of **3**. The amount of **3** which decomposes is 87 to 100% based on line broadening on the ^{51}P NMR lines and cathodic stripping. The deposition of Co on the electrode surface is the same as was reported earlier by the group of Nocera.[59]

The development of the Co_4-POM systems **2** and **3** have led to a heated discussion in the literature with regard to the homogeneity and the structure of the active catalyst.[47, 48, 52, 53, 55–58] At low concentration, **2** forms a stable complex under (photo)chemical water oxidation conditions,[47, 52] at higher concentrations and under electrochemical water oxidation conditions it forms a metal oxide deposit on the electrode surface.[48] Although $[Ru(bpy)_3]^{3+}$ is not capable of oxidizing **2**, depletion of $[Ru(bpy)_3]^{3+}$ is observed in laser flash photolysis experiments, indicating that **2** decomposes to form a molecular complex with a lower oxidation potential in phosphate buffer.[53] The Co_4-POM **3** is believed not to be structurally correct but decomposes rapidly to form CoO_x under electrochemical conditions which is responsible for the water oxidation catalysis.[57, 58] Due to the harsh conditions of water oxidation catalysis, similar systems with homogeneous catalyst must suffer from stability issues as well, although this is often neglected in electrochemical studies.

1.3 Homogeneous *versus* heterogeneous electrochemical water oxidation and oxygen reduction catalysis concerning molecular (pre)catalysts

1.3.1 Scope of this thesis

The formation of heterogeneous materials from homogeneous (pre)catalysts is not unique to the Co-POM systems. However there are few reports of molecular complexes forming heterogeneous catalysts under reactive conditions. The aim of this thesis is to investigate the mechanism

of the formation of heterogeneous layers under catalytic conditions and strategies to prevent the formation of metal(oxide) deposits on electrodes under catalytic conditions. The focus is on the difficult but important water oxidation and oxygen reduction reactions, which form the bottleneck for the efficient storage of renewable energy in a chemical bond.

In Chapter 2 the water oxidation reaction is reported with two similar pyridyl-triazolylidene iridium complexes, which differ only in one position on the pyridyl-triazolylidene ligand. The influence of the ligand structure on the activity and the activation of the catalytic system has been investigated electrochemically. An *in situ* study on the formation of surface deposits and the gaseous products has been performed, while *ex situ* spectroscopy was used to investigate the structure and nature of the active site.

Copper complexes display rapid ligand exchange kinetics. The exchange rate of water ligands at Cu^{II} complexes is in the order of 10^8 s^{-1}.[46, 60] This is faster than the exchange rate on other first row transition metals such as Fe^{II} (10^5 s^{-1}), Co^{II} (10^4 s^{-1}) and Mn^{II} (10^5 s^{-1}). The exchange rate of water on noble metals is lower, with Ir^{III} having the slowest exchange rate (10^{-6} s^{-1}). The fast exchange kinetics of water ligands at Cu^{II} centers indicates that also other ligands will exchange more rapidly at copper complexes compared to other metals. Therefore care should be taken when using Cu^{II} complexes in the water oxidation and oxygen reduction reactions, as free Cu^{II} may be present already at very early stages during the catalytic reaction.

In Chapter 3 a $[Cu^{II}(bdmpza)_2]$ complex (bdmpza$^-$ = bis(3,5-dimethyl-1H-pyrazol-1-yl)acetate has been investigated for the water oxidation reaction. The exchange of the ligands with water or ions present in the electrolyte is minimized by the use of a tridentate bis-pyrazole ligand. The formation of a CuO layer was, however, not prevented, but even faster obtained if the complex was first treated under reducing conditions.

In Chapter 4 *in situ* generated Cu^{II} complexes with 1,10-phenanthroline ligands are reported for the oxygen reduction reaction. The use of a high concentration of 1,10-phenanthroline, should shift the equilibrium of phenanthroline binding towards complex formation, thus preventing the formation of metallic copper on the electrode surface.

Chapter 5 reports copper complexes with 1,10-phenanthrolineligands which are covalently attached to the electrode surface while Cu^{II} is present in the electrolyte solution. In presence of copper, $[Cu(phen)L_x]$ complexes form on the surface of the gold working electrode. By immo-

bilizing the ligands onto the electrode surface, the copper ions cannot get close to the electrode surface. The formation of metallic copper on the electrode surface under oxygen reduction conditions is prevented by blocking of the ligands which are attached to the electrode surface. The *in situ* generated copper complexes have been investigated for the oxygen reduction reaction.

1.4 References

(1) Carbon Dioxide | Vital Signs – Climate Change: Vital Signs of the Planet., https://climate.nasa.gov/vital-signs/carbon-dioxide/, Accessed: 2018-08-06.

(2) US Department of Commerce, NOAA, E. S. R. L. ESRL Global Monitoring Division - Global Greenhouse Gas Reference Network., https://www.esrl.noaa.gov/gmd/ccgg/trends/full.html, Accessed: 2018-08-06.

(3) OMR - OMR Public., https://www.iea.org/oilmarketreport/omrpublic/, Accessed: 2018-08-06.

(4) Global Temperature | Vital Signs – Climate Change: Vital Signs of the Planet., https://climate.nasa.gov/vital-signs/global-temperature/, Accessed: 2018-08-06.

(5) Ellabban, O.; Abu-Rub, H.; Blaabjerg, F. *Renew. Sust. Energ. Rev.* **2014**, *39*, 748–764.

(6) Jacobson, M. Z.; Delucchi, M. A. *Energy Policy* **2011**, *39*, 1154–1169.

(7) Zeradjanin, A. R.; Grote, J.-P.; Polymeros, G.; Mayrhofer, K. J. J. *Electroanal.* **2016**, *28*, 2256–2269.

(8) Zeng, M.; Li, Y. *J. Mater. Chem. A* **2015**, *3*, 14942–14962.

(9) Pedersen, C. M.; Escudero-Escribano, M.; Velázquez-Palenzuela, A.; Christensen, L. H.; Chorkendorff, I.; Stephens, I. E. L. *Electrochim. Acta* **2015**, *179*, 647–657.

(10) Davydova, E. S.; Mukerjee, S.; Jaouen, F.; Dekel, D. R. *ACS Catal.* **2018**, *8*, 6665–6690.

(11) Lu, S.; Zhuang, Z. *Sci. China Mater.* **2016**, *59*, 217–238.

(12) Kibsgaard, J.; Gorlin, Y.; Chen, Z.; Jaramillo, T. F. *J. Am. Chem. Soc.* **2012**, *134*, 7758–7765.

(13) Ostwald, F. W. *Nature* **1902**, *65*, 522–526.

(14) Crabtree, R. H. *Chem. Rev.* **2012**, *112*, 1536–1554.

(15) Hessels, J.; Detz, R. J.; Koper, M. T. M.; Reek, J. N. H. *Chem. Eur. J.* **2017**, *23*, 16413–16418.

(16) Hunter, B. M.; Gray, H. B.; Müller, A. M. *Chem. Rev.* **2016**, *116*, 14120–14136.

(17) Roger, I.; Shipman, M. A.; Symes, M. D. *Nat. Rev. Chem.* **2017**, *1*, 1–13.

(18) Rüttinger, W.; Dismukes, G. C. *Chem. Rev.* **1997**, *97*, 1–24.

(19) McCrory, C. C. L.; Jung, S.; Peters, J. C.; Jaramillo, T. F. *J. Am. Chem. Soc.* **2013**, *135*, 16977–16987.

(20) Koper, M. T. M. *J. Electroanal. Chem.* **2011**, *660*, 254–260.

(21) Fernández, E. M.; Moses, P. G.; Toftelund, A.; Hansen, H. A.; Martínez, J. I.; Abild-Pedersen, F.; Kleis, J.; Hinnemann, B.; Rossmeisl, J.; Bligaard, T.; Nørskov, J. K. *Angew. Chem. Int. Ed.* **2008**, *47*, 4683–4686.

(22) Rossmeisl, J.; Qu, Z.-W.; Zhu, H.; Kroes, G.-J.; Nørskov, J. K. *J. Electroanal. Chem.* **2007**, *607*, 83–89.

(23) Sala, X.; Maji, S.; Bofill, R.; García-Antón, J.; Escriche, L.; Llobet, A. *Acc. Chem. Res.* **2014**, *47*, 504–516.

(24) Gersten, S. W.; Samuels, G. J.; Meyer, T. J. *J. Am. Chem. Soc.* **1982**, *104*, 4029–4030.

(25) Duan, L.; Araujo, C. M.; Ahlquist, M. S. G.; Sun, L. *P. Natl, Acad. Sci. U.S.A.* **2012**, *109*, 15584–15588.

(26) Duan, L.; Bozoglian, F.; Mandal, S.; Stewart, B.; Privalov, T.; Llobet, A.; Sun, L. *Nat. Chem.* **2012**, *4*, 418–423.

(27) McDaniel, N. D.; Coughlin, F. J.; Tinker, L. L.; Bernhard, S. *J. Am. Chem. Soc.* **2008**, *130*, 210–217.

(28) Blakemore, J. D.; Crabtree, R. H.; Brudvig, G. W. *Chem. Rev.* **2015**, *115*, 12974–13005.

(29) Hetterscheid, D. G. H.; Reek, J. N. H. *Eur. J. Inorg. Chem.* **2014**, 742–749.

(30) Hetterscheid, D. G. H. *Chem. Commun.* **2017**, *53*, 10622–10631.

(31) Blakemore, J. D.; Schley, N. D.; Olack, G. W.; Incarvito, C. D.; Brudvig, G. W.; Crabtree, R. H. *Chem. Sci.* **2011**, *2*, 94–98.

(32) Abril, P.; del Rio, M. P.; Tejel, C.; Verhoeven, T. W. G. M.; Niemantsverdriet, J. W.; Van der Ham, C. J. M.; Kottrup, K. G.; Hetterscheid, D. G. H. *ACS Catal.* **2016**, *6*, 7872–7875.

(33) Schley, N. D.; Blakemore, J. D.; Subbaiyan, N. K.; Incarvito, C. D.; D'Souza, F.; Crabtree, R. H.; Brudvig, G. W. *J. Am. Chem. Soc.* **2011**, *133*, 10473–10481.

(34) Van Dijk, B.; Hofmann, J. P.; Hetterscheid, D. G. H. *Phys. Chem. Chem. Phys.* **2018**, *20*, 19625–19634.

(35) Thorum, M. S.; Yadav, J.; Gewirth, A. A. *Angew. Chem. Int. Ed.* **2009**, *48*, 165–167.

(36) Xi, Y.-T.; Wei, P.-J.; Wang, R.-C.; Liu, J.-G. *Chem. Commun.* **2015**, *51*, 7455–7458.

(37) Zhang, T.; Wang, C.; Liu, S.; Wang, J.-L.; Lin, W. *J. Am. Chem. Soc.* **2014**, *136*, 273–281.

(38) Su, X.-J.; Gao, M.; Jiao, L.; Liao, R.-Z. Z.; Siegbahn, P. E. M.; Cheng, J.-P.; Zhang, M.-T. *Angew. Chem. Int. Ed.* **2015**, *54*, 4909–4914.

(39) Barnett, S. M.; Goldberg, K. I.; Mayer, J. M. *Nat. Chem.* **2012**, *4*, 498–502.

(40) Fisher, K. J.; Materna, K. L.; Mercado, B. Q.; Crabtree, R. H.; Brudvig, G. W. *ACS Catal.* **2017**, *7*, 3384–3387.

(41) Zhang, J.; Anson, F. C. *Electrochim. Acta* **1993**, *38*, 2423–2429.

(42) Zhang, J.; Anson, F. C. *J. Electroanal. Chem.* **1992**, *341*, 323–341.

(43) Lei, Y.; Anson, F. C. *Inorg. Chem.* **1994**, *33*, 5003–5009.

(44) Langerman, M. P.; Hetterscheid, D. G. H. *Submitted*.

(45) Asahi, M.; Yamazaki, S.-i.; Itoh, S.; Ioroi, T. *Dalton T.* **2014**, *43*, 10705.

(46) Reedijk, J. *Platin. Met. Rev.* **2008**, *52*, 2–11.

(47) Yin, Q.; Tan, J. M.; Besson, C.; Geletii, Y. V.; Musaev, D. G.; Kuznetsov, A. E.; Luo, Z.; Hardcastle, K. I.; Hill, C. L. *Science* **2010**, *328*, 342–5.

(48) Stracke, J. J.; Finke, R. G. *J. Am. Chem. Soc.* **2011**, *133*, 14872–14875.

(49) Geletii, Y. V.; Botar, B.; Kögerler, P.; Hillesheim, D. A.; Musaev, D. G.; Hill, C. L. *Angew. Chem. Int. Ed.* **2008**, *47*, 3896–3899.

(50) Sartorel, A.; Carraro, M.; Scorrano, G.; De Zorzi, R.; Geremia, S.; McDaniel, N. D.; Bernhard, S.; Bonchio, M. *J. Am. Chem. Soc.* **2008**, *130*, 5006–5007.

(51) Geletii, Y. V.; Besson, C.; Hou, Y.; Yin, Q.; Musaev, D. G.; Quiñonero, D.; Cao, R.; Hardcastle, K. I.; Proust, A.; Kögerler, P.; Hill, C. L. *J. Am. Chem. Soc.* **2009**, *131*, 17360–17370.

(52) Huang, Z.; Luo, Z.; Geletii, Y. V.; Vickers, J. W.; Yin, Q.; Wu, D.; Hou, Y.; Ding, Y.; Song, J.; Musaev, D. G.; Hill, C. L.; Lian, T. *J. Am. Chem. Soc.* **2011**, *133*, 2068–2071.

(53) Natali, M.; Berardi, S.; Sartorel, A.; Bonchio, M.; Campagna, S.; Scandola, F. *Chem. Commun.* **2012**, *48*, 8808.

(54) Natali, M.; Orlandi, M.; Berardi, S.; Campagna, S.; Bonchio, M.; Sartorel, A.; Scandola, F. *Inorg. Chem.* **2012**, *51*, 7324–7331.

(55) Vickers, J. W.; Lv, H. J.; Sumliner, J. M.; Zhu, G. B.; Luo, Z.; Musaev, D. G.; Geletii, Y. V.; Hill, C. L. *J. Am. Chem. Soc.* **2013**, *135*, 14110–14118.

(56) Lv, H.; Song, J.; Geletii, Y. V.; Vickers, J. W.; Sumliner, J. M.; Musaev, D. G.; Kögerler, P.; Zhuk, P. F.; Bacsa, J.; Zhu, G.; Hill, C. L. *J. Am. Chem. Soc.* **2014**, *136*, 9268–9271.

(57) Folkman, S. J.; Kirner, J. T.; Finke, R. G. *Inorg. Chem.* **2016**, *55*, 5343–5355.

(58) Folkman, S. J.; Finke, R. G. *ACS Catal.* **2017**, *7*, 7–16.

(59) Kanan, M. W.; Nocera, D. G. *Science* **2008**, *321*, 1072–1075.

(60) Taube, H. *Chem. Rev.* **1952**, *50*, 69–126.